International Journal of Computational Intelligence Systems
Vol. **14(1)**, 2021, *pp.* 537–549
DOI: https://doi.org/10.2991/ijcis.d.201228.002; ISSN: 1875-6891; eISSN: 1875-6883
https://www.atlantis-press.com/journals/ijcis/

Research Article

Fault Diagnosis of Bearings Using an Intelligence-Based Autoregressive Learning Lyapunov Algorithm

Farzin Piltan[1], Jong-Myon Kim[2,*]

[1] *Department of Electrical, Electronics and Computer Engineering, University of Ulsan, Ulsan, 680-479, Korea*
[2] *School of IT Convergence, University of Ulsan, Ulsan, 680-479, Korea*

ARTICLE INFO

Article History

Received 27 Oct 2020
Accepted 21 Dec 2020

Keywords

Lyapunov-based observer
Fuzzy algorithm
Adaptive technique
Autoregressive learning signal modeling
Support vector regression
Support vector machine
Fault diagnosis

ABSTRACT

Bearings are complex components with nonlinear behavior that are used to reduce the effect of inertia. They are used in applications such as induction motors and rotating components. Condition monitoring and effective data analysis are important aspects of fault detection and classification in bearings. Thus, an effective and robust hybrid technique for fault detection and identification is presented in this study. The proposed scheme has four main steps. First, a mathematical approach is combined with an autoregressive learning technique to approximate the vibration signal under normal conditions and extract the state-space equation. In the next step, an intelligence-based observer is designed using a combination of the robust Lyapunov-based method, autoregressive learning scheme, fuzzy technique, and adaptive algorithm. The intelligence-based observer is the main part of the algorithm that determines the fault estimation in the bearing. After estimating the signals, in the third step, the residual signals are generated, resampled, and the root mean square (RMS) is extracted from the resampled residual signals. Then, in the final step, the classification, detection, and identification of the signal is performed by the support vector machine algorithm. The effectiveness of the proposed learning control algorithm is analyzed using the Case Western Reverse University (CWRU) bearing vibration dataset. The proposed method is compared to two state-of-the-art techniques: an autoregressive learning Lyapunov-based observer and a Lyapunov-based observer. The proposed algorithm improved the average fault identification accuracy by 3.9% and 5.2% compared to the autoregressive learning Lyapunov-based approach and the Lyapunov-based technique, respectively.

1. INTRODUCTION

Bearings are generally used in rotary machines to reduce friction. Bearings are used extensively in various industries, such as petroleum, automotive, and robotics. They are vulnerable due to high operating loads and rotational speeds. Thus, early detection of faults in these components is exceedingly important [1,2]. In general, bearings are exposed to four types of defects: inner, outer, ball, and cage. Among these faults, outer defects have the highest reproducibility in bearings [2,3]. Different methods are used to detect and analyze bearing faults, but regardless of the type of fault detection algorithm, the first step is data collection. Techniques that have been prescribed for condition monitoring in bearings include vibration signals, acoustic emission signals, and motor current signature analysis (MCSA) signals [2,3].

Identifying and isolating different faults occurs as part of system condition monitoring, which is a subset of control engineering. There are three basic methods for fault detection and identification in bearings. The first method comprises data-driven techniques that use the sensor's data alone and analyze this information using signal processing algorithms and machine/deep learning techniques. The second approach is model-based, and uses the difference between the data extracted from sensors and the system's model. Finally, hybrid techniques use a combination of the data-driven and model-based methods [1–3].

Model-based and data-driven techniques each have their own advantages and disadvantages for bearing fault detection and identification [4,5]. The main challenges of data-driven approaches are the dependence on data collection from the bearing and the reliability required for use in industry. The main impediments of model-based procedures are the flexibility and complexity of system modeling required, especially for complex industrial systems [5–9]. Thus, to avoid the limitations of data-driven and model-based approaches, hybrid techniques are employed. These techniques have been recommended by several researchers, and include combined signal processing and machine learning approaches, or combined model-based approaches and artificial intelligence methods. In this study, model-based, machine learning, and data-driven schemes are combined for fault detection and identification in bearings [10–14].

In recent years, researchers have published various articles on the application of model-based techniques for fault diagnosis. These techniques can be divided into two groups: linear maneuverings

* *Corresponding author. Email: jongmyon.kim@gmail.com*

and nonlinear procedures [13–15]. Regardless of whether an algorithm is linear or nonlinear, the first step is to calculate a mathematical model of the system, either directly or indirectly. In the direct modeling method, the mathematical model of the system is extracted from the dynamic behavior of the system using a technique such as Newton-Euler or Lagrange methods. In the indirect method, the mathematical model of the system is estimated from the input-output signals collected by the sensors. System identification approaches are one of the most important indirect modeling procedures. These techniques are generally divided into two categories: linear and nonlinear. Autoregressive or autoregressive-Laguerre models are classified as linear modeling techniques [16–18]. The artificial intelligence methods including various kinds of neural networks and fuzzy logic techniques have been recommended for nonlinear system modeling [19–21]. Such recent applications pointed out in [22] include the novel interval-valued spherical fuzzy sets for the highly nonlinear system [19], an incremental online identification algorithm to develop a set of evolving fuzzy models (FMs) [20], modeling and classification the nonlinear systems based on artificial neural network and hidden Markov model [21], evolving FMs [22], prediction of system's behavior from the signals by extreme learning machines [23], and the combination of nonlinear autoregressive with exogenous inputs and variable structure recurrent dynamic neural networks [24]. A combination of linear system modeling techniques and intelligent procedures are selected for mathematical modeling of the nonlinear and complex systems. To increase the accuracy and reliability of bearing modeling, mathematical modeling of vibration signals and a nonlinear system identification technique with a combination of an autoregressive algorithm, Laguerre filter method, and support vector regression (SVR) is recommended in this work.

After extracting the mathematical formulation of the bearing vibration signal in the normal state, a dynamic system called an estimator is used to solve modeling problems in the state space such as not having access to all variables, impractical measurement of all variables, and high measurement cost. In general, estimators are divided into two main categories: full-order estimators and reduced-order estimators [25–30]. In the full-order estimator, the estimator degree is equal to the system's degree, while in the reduced-order estimator, the estimator degree is less than that of the system, thereby reducing the number of variables. Estimators can be designed linearly or nonlinearly. For example, in a linear proportional-integral (PI) estimator, two variables are considered to reduce the estimation error [18,30], whereas in a nonlinear feedback linearization estimator, the number of variables are increased, and a nonlinear function is extracted from the nonlinear system model to reduce the error. Severe dependency on the system's dynamic model is the most consequential difficulty of the feedback linearization estimator [29]. Other candidates for solving the problems of the feedback back linearization estimator are the sliding mode estimation and backstepping estimation procedures [28]. The use of these techniques reduces the dependency of the estimator on the system's dynamics. However, the sliding mode technique has the challenge of high-frequency fluctuations that increase the error rate, and the backstepping technique lacks robustness in uncertain conditions. To avoid the above challenges, this article uses Lyapunov's robust, reliable, and stable estimator. This technique provides a stable scheme for impulsive signals. In the normal case, the solution of impulsive signals requires investigation by solving partial differential equations, whereas in the Lyapunov case, simpler methods can used. Lyapunov's technique also solves the challenge of stability in the transient state. Furthermore, the multi autoregressive learning technique solves the problem of nonlinear and nonstationary signal modeling in the Lyapunov estimator. Moreover, the adaptive fuzzy algorithm can be used in combination with the multi autoregressive learning technique and the Lyapunov approach to increase the flexibility as well as the reliability, stability, and robustness. Then, in this article, the adaptive fuzzy-based autoregressive learning Lyapunov algorithm is combined with the support vector machine (SVM) for fault estimation, detection, and identification. To achieve these goals, there are three steps, as shown in Figure 1. The first step is approximation of the normal vibration signal using the combination of autoregressive learning and mathematical vibration modeling. In the second step, normal and abnormal signals are estimated using an adaptive fuzzy-based autoregressive learning Lyapunov algorithm. In the third step, faults are detected and identified using a combination of an adaptive fuzzy-based autoregressive learning Lyapunov algorithm and SVM. As shown in Figure 1, the goal of the first step is to model the vibration signal in the normal condition (NRM).

Therefore, first, mathematical modeling of the vibration signal with five degrees of freedom (DOF) is recommended. Additionally, the autoregression technique is used to mathematically model the normal vibration signal. In the next step, the autoregressive technique must be strengthened; this is done using the Laguerre input-output filter. Then, the accuracy of the modeling is increased by SVR. Therefore, by combining autoregressive learning, Laguerre filter, and SVR, the bearing vibration signal is modeled in the NRM. In the second step shown in Figure 1, the main goal is to design a robust, stable, and flexible estimator. Therefore, first, the Lyapunov estimator is suggested.

To overcome the nonlinear part of the vibration signal, the autoregressive learning technique from the modeling part is added to this part and strengthens the signal estimation property. The combination of TSK fuzzy algorithm with the Lyapunov autoregressive learning technique is used to reduce the challenge of uncertainties.

Finally, an adaptive procedure is combined with the fuzzy Lyapunov autoregressive learning technique to increase the flexibility and the quality of the estimation. As shown in Figure 1, fault detection and identification occur in the last step. In this step, first, the residual signal is calculated as the difference between the original and estimated signals. Next, the amount of the signal's root means square (RMS) is determined; finally, the RMS of the residual signal is identified by classification algorithms such as SVM. This article has the following contributions:

- The combination of mathematical-based vibration signal modeling and autoregressive learning techniques is used for vibration signal approximation of a bearing.
- The adaptive fuzzy autoregressive learning Lyapunov scheme is suggested for signal estimation in different conditions.
- The combination of mathematical-based vibration signal modeling and autoregressive learning techniques for vibration signal approximation, the adaptive fuzzy autoregressive

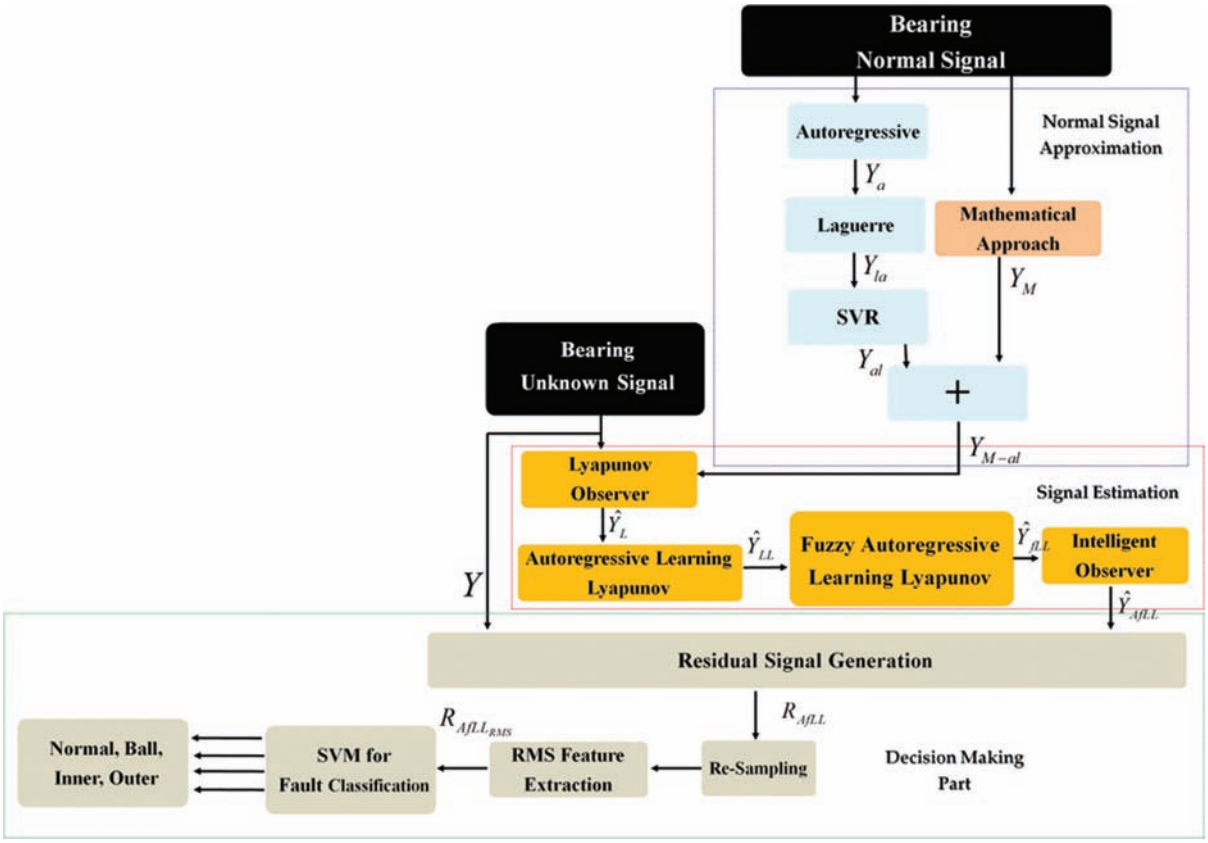

Figure 1 | The artificial-based observer, combination of the mathematical-autoregressive learning modeling, and support vector machine for fault detection and identification.

learning Lyapunov scheme for signal estimation, and SVM for classification of bearing fault in one frame.

The structure of this article is as follows: The Case Western Reverse University (CWRU) bearing dataset is described in the second section. In the third section, the vibration signals for the NRM are modeled using the combination of mathematical-based vibration signal modeling and autoregressive learning techniques. The proposed adaptive fuzzy autoregressive learning Lyapunov algorithm for signal estimation, the vibration residual signal generation, determination of the RMS of residual signals, and classification using SVM for fault detection and identification are explained in the fourth section. The results are discussed in Section 5. Finally, the conclusions are provided in Section 6.

2. DATASET

The CWRU dataset is selected to test the proposed scheme and compare it with two state-of-the-art algorithms. In the CWRU dataset, a 2-horsepower (hp) induction motor is utilized to rotate the bearing at various speeds. A vibration sensor collects normal and abnormal vibration signals with a sampling rate of 48 kHz. The bearing used in the CWRU dataset is the 6205-2RS JEM SKF roller bearing; its parameters are given in Table 1. In this dataset, four different classes are defined: NRM, ball fault (BLF), inner race fault (IRF), and outer race fault (ORF). The vibration signal in the NRM is modeled and estimated at 0-hp. Then, the normal signal

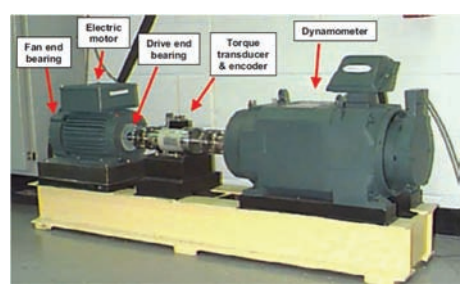

Figure 2 | Case Western Reverse University (CWRU) data collection center [28].

and abnormal signals with 0.007-inch, 0.014-inch, and 0.021-inch crack sizes are recorded for 0-hp, 1-hp, 2-hp, and 3-hp torque loads. Figure 2 shows the CWRU test bench for data collection. Table 2 shows the data description for the CWRU dataset in normal and abnormal states [31].

3. SIGNAL MODELING

In this section, the vibration signal of the bearing in the NRM is modeled using five DOF mathematical modeling of the vibration signal and autoregressive learning algorithm. The mathematical technique (MAT) is a reliable algorithm for modeling the bearing, but it has limitations in an uncertain state. The combination of

Table 1 Parameters of Case Western Reverse University (CWRU) bearing for mathematical modeling [29].

Parameters	Value
Number of balls	9
Stiffness of ball	$5.96 \times 10^7 \left(\frac{N}{m}\right)$
Mass of outer (kg)	2.7(Kg)
Stiffness of outer	$1.31 \times 10^5 \left(\frac{N}{m}\right)$
Mass of shaft (kg)	1.36(Kg)
Stiffness of shaft	$23.3 \times 10^6 \left(\frac{N}{m}\right)$
Damping	$654 \left(\frac{NS}{m}\right)$
Ball diameter	7.940(mm)
Pitch diameter	39.04 (mm)
Defect size	7 (mm)
Defect depth	2(mm

Table 2 Case Western Reserve University (CWRU) vibration datasets [28,29].

Dataset Group	C	Load (hp)	Crack Sizes (in)
i	NRM	0	0.007, 0.014, and 0.021
	BLF	0	
	IRF	0	
	ORF	0	
ii	NRM	1	0.007, 0.014, and 0.021
	BLF	1	
	IRF	1	
	ORF	1	
iii	NRM	2	0.007, 0.014, and 0.021
	BLF	2	
	IRF	2	
	ORF	2	
iv	NRM	3	0.007, 0.014, and 0.021
	BLF	3	
	IRF	3	
	ORF	3	

NRM, normal condition; BLF, ball fault; IRF, inner race fault; ORF, outer race fault.

autoregressive and machine learning techniques is prescribed to increase the accuracy under uncertain conditions [28,29].

3.1. Mathematical Modeling of Bearing

The mathematical modeling of a 5-DOF vibration signal under NRMs in the bearing is expressed by the following equation:

$$f_{(q)} = M_{(q)}[\ddot{q}] + B(q, \dot{q}) + \Delta \tag{1}$$

Here, $f_{(q)}, M_{(q)}, \ddot{q}, B(q, \dot{q})$, and Δ are the force of bearing, the mass matrix of the bearing, the acceleration, the nonlinear term for mathematical modeling of the bearing, and uncertainty, respectively. The nonlinear term is defined by the following equation:

$$B(q, \dot{q}) = S_{(q)}[\dot{q}] + D_{(q)}[q] \tag{2}$$

Here, $S_{(q)}, \dot{q}$, and $D_{(q)}$ are the time variant stiffness, the velocity, and the damping matrices, respectively. One of the main problems in mathematical modeling of systems is the issue of how to estimate the uncertainty. It is unavoidably laborious, and sometimes it is almost impossible to obtain an accurate approximation. Based on [28], the uncertainties can be modeled with 5-DOF using the following technique:

$$\Delta = \Theta_b + \Theta_i + \Theta_o \tag{3}$$

Here, Θ_b, Θ_i, and Θ_o are the predicted ball effect, predicted inner effect, and predicted outer effect, respectively. The predicted ball effect (Θ_b) is represented by the following function:

$$\Theta_b = Max\left(\Theta_{xd} Cos\left(\Theta_j\right) + \Theta_{xd} Sin\left(\Theta_j\right) - C_\omega - \Theta_f, 0\right) \tag{4}$$

Here, (Θ_{xd}) is the difference between the inner and outer centers of mass.

$$\Theta_{xd} = \Theta_{xi} - \Theta_{xo} \tag{5}$$

The ball angular position is defined as

$$\Theta_j = \frac{2\pi(j-1)}{b_n} + C_\omega + \Theta_o \tag{6}$$

where Θ_j, b_n, C_ω, and Θ_o are the angular position of the ball, the number balls, the velocity of the rotor, and the initial position of the ball, respectively. The fault deformation is defined as follows:

$$\Theta_f = C_{\omega_a} + C_{\omega_b} \tag{7}$$

Here, C_{ω_a} and C_{ω_b} are the angular width at position a and the angular width at position b, respectively. Moreover, the predictions of the inner (Θ_i) and outer (Θ_o) effects are represented by the following functions, respectively:

$$\Theta_i = Max\left(\Theta_{xd} Cos\left(\Theta_j\right) - \Theta_{xd} Sin\left(\Theta_j\right) - \left(2 \times \left(C_\omega - \Theta_f\right)\right), 0\right) \tag{8}$$

$$\Theta_o = Max\left(\Theta_{xd} Cos\left(\Theta_j\right) + 1.5 \times \Theta_{xd} Sin\left(\Theta_j\right) - C_\omega + \Theta_f, 0\right) \tag{9}$$

Therefore, the state-space mathematical modeling of the bearing is represented as the following equation:

$$\begin{cases} X_M(k+1) = \alpha_M\left(X_M(k), U(k)\right) + \Delta\left(X_M(k), U(k)\right) \\ Y_M(k) = (\alpha_G)^T X_M(k) \end{cases} \tag{10}$$

Here, $X_M(k), U(k), \alpha_M\left(X_M(k), U(k)\right), Y_M(k), \alpha_G$, and $\Delta\left(X_M(k), U(k)\right)$ are the state of vibration signal, the input measurable vibration signal, the nonlinear term of signal modeling using vibration signal, the output measurable vibration signal, the coefficient of signal approximation, and uncertainties in the NRM, respectively. After mathematical modeling of the bearing based on the vibration signal, the autoregressive learning algorithm is used to improve the accuracy of the signal estimation.

3.2. Autoregressive Learning Algorithm for Bearing Signal Approximation

The core of this work is the design of an artificial intelligence-based observer to identify bearing faults using an estimation algorithm. Thus, the first step is to extract the state-space equation from the bearing vibration signal. Therefore, the autoregressive technique in combination with Laguerre bearing signal filter and support vector regression (SVR) that from now on, it will be called autoregressive learning technique is introduced. The first step is modeling the bearing vibration signal using the autoregressive algorithm [24].

$$\begin{cases} X_a(k+1) = [\alpha_a X_a(k) + \alpha_{ai} U_{ai}(k)] + e_a(k) + f(k) \\ Y_a(k) = (\alpha_o)^T X_a(k) \end{cases} \tag{11}$$

Here, $X_a(k)$, $U_{ai}(k)$, $e_a(k)$, $f(k)$, $Y_a(k)$, and $(\alpha_a, \alpha_{ai}, \alpha_o)$ are the state of bearing vibration signal using autoregressive technique, the input measurable state of bearing vibration signal, the error of bearing vibration signal modeling using the autoregressive technique, the uncertainties in the NRM, the output measurable state of the bearing vibration signal using the autoregressive technique, and the coefficients for state, input, and output, respectively. The error of signal modeling based on the autoregressive technique for vibration signal is defined using the following equation:

$$e_a(k) = Y_a(k+1) - Y_a(k) \tag{12}$$

To improve the robustness of the autoregressive technique, the Laguerre algorithm is recommended [30]. The Laguerre-autoregressive filter technique and the error are represented by the following state-space algorithms [28,29].

$$\begin{cases} X_{la}(k+1) = [\alpha_a X_{la}(k) + \alpha_{ai} U_{ai}(k) + \alpha_{lao} Y_{la}(k)] + e_{la}(k) + f(k) \\ Y_{la}(k) = (\alpha_o)^T X_{la}(k) \end{cases} \tag{13}$$

$$e_{la}(k) = Y_{la}(k+1) - Y_{la}(k) \tag{14}$$

Here, $X_{la}(k)$, $e_{la}(k)$, $Y_{la}(k)$ and (α_{lao}) are the state of bearing vibration signal using the Laguerre-autoregressive technique, the error of bearing vibration signal modeling using the Laguerre-autoregressive technique, the output measurable state of bearing vibration signal using the Laguerre-autoregressive technique, and the coefficient of the Laguerre-autoregressive technique for output, respectively. The foremost difficulty in designing nonlinear observation techniques such as a Lyapunov observer is estimating the nonlinear dynamic parameters. Accurate nonlinear term modeling of bearings is very difficult, so a nonlinear function approximation technique is recommended. The SVR is a learning technique to approximate the vibration bearing signal. Therefore, the combination of SVR and the Laguerre-autoregressive technique is recommended for nonlinear vibration signal approximation in this research. The basic concept of this technique is the learning algorithm. Nonlinear regression based on the SVR and using the kernel trick is defined by the following equation [32,33]:

$$Y_{SVR} = \sum_i \left(\alpha_i^+ - \alpha_i^-\right) K(x_i, x) + b \tag{15}$$

Here, Y_{SVR}, $\left(\alpha_i^+, \alpha_i^-\right)$, $K(x_i, x)$, and b are the output modeled flowrate based on SVR, the Lagrange coefficients, the kernel, and the bias, respectively. Various functions can be introduced as kernel functions; in this work, the Gaussian function is defined as follows:

$$K(x_i, x) = e^{\left(-\frac{1}{2\sigma^2}\|x_i - x\|^2\right)} \tag{16}$$

Here, σ is variance. To solve it, the minimum of $\left(\alpha_i^+, \alpha_i^-\right)$ is calculated by the following technique:

$$\min \sum_i \sum_j \left(\alpha_i^+ - \alpha_i^-\right)\left(\alpha_i^+ - \alpha_i^-\right) K(x_i, x) \tag{17}$$

Then $K(x_i, x)$ is defined by w_{ij} and

$$\min \sum_i \sum_j \alpha_i^+ \alpha_i^+ w_{ij} - \alpha_i^- \alpha_i^+ w_{ij} - \alpha_i^+ \alpha_i^- w_{ij} + \alpha_i^- \alpha_i^- w_{ij} \tag{18}$$

While

$$W = \left[w_{ij}\right] \in \mathbb{R}^{n \times n}$$

$$\alpha = \begin{bmatrix} \alpha^+ \\ \alpha^- \end{bmatrix}_{2n \times 1}$$

$$\varpi = \begin{bmatrix} W & -W \\ -W & W \end{bmatrix}$$

Therefore, the above formulation is rewritten as

$$\min \frac{1}{2} \alpha^T \varpi \alpha + \kappa^T \alpha \tag{19}$$

if $\kappa = \begin{bmatrix} -Y + \varepsilon \\ Y + \varepsilon \end{bmatrix}_{2n \times 1}$. Here Y and ε are the vibration bearing signal measured by vibration sensors and accepted boundary of modeling.

$$\sum_i \left(\alpha_i^+ - \alpha_i^-\right) = 0 \tag{20}$$

Thus, the bias is calculated using the following equation:

$$b = \frac{1}{|S|} \sum_{s \in S} \left[Y_s - \sum_{i \in S} \left(\alpha_i^+ - \alpha_i^-\right) \times K(x_i, x_S) - \varepsilon \times sign\left(\alpha_i^+ - \alpha_i^-\right) \right] \tag{21}$$

Here, Y_s and S are vibration of support vector and support vector, respectively. The support vector is defined by the following equation:

$$S = \left\{ i | 0 < \alpha_i^+ + \alpha_i^- < \delta \right\} \tag{22}$$

Here, δ is a constant. Therefore, the combination of SVR and Laguerre-autoregressive (autoregressive learning) algorithm is represented by the following definition:

$$\begin{cases} X_{al}(k+1) = [\alpha_a X_{al}(k) + \alpha_{ai} U_{ai}(k) + \alpha_{lao}(Y_{la}(k) \\ \qquad + Y_{SVR}(k) + e_{al}(k) + f(k) \\ Y_{al}(k) = (\alpha_o)^T X_{al}(k) \end{cases} \tag{23}$$

$$e_{al}(k) = Y_{al}(k+1) - Y_{al}(k) \tag{24}$$

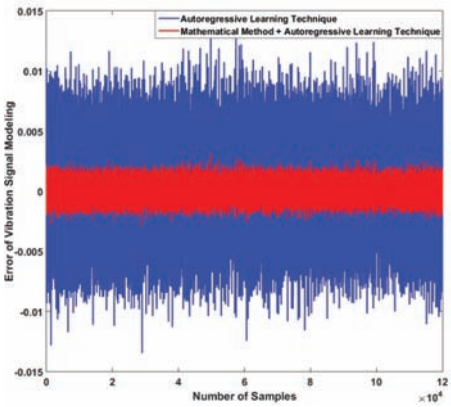

Figure 3 | Error of bearing modeling using autoregressive learning technique and the combination of mathematical system modeling and autoregressive learning approach.

Here, $X_{al}(k)$, $e_{al}(k)$, $Y_{al}(k)$, and (Y_{SVR}) are the state of bearing vibration signal using autoregressive learning technique, the error of bearing vibration signal modeling using autoregressive learning technique, the output measurable state of the bearing vibration signal using autoregressive learning technique, and the output measurable state of bearing vibration signal using SVR technique, respectively. Thus, regarding the state-space system modeling techniques using MAT (Eq. 10) and autoregressive learning technique (Eq. 23), the combination of these two techniques and the mean square error of the proposed signal modeling scheme are represented as the following formulation:

$$\begin{cases} X_{M-al}(k+1) = X_M(k+1) + X_{al}(k+1) \\ Y_{M-al}(k) = Y_M(k) + Y_{al}(k) \\ MSE = \dfrac{1}{k}\displaystyle\sum_{1}^{k}(Y_{M-al}(k) - Y(k)) \end{cases} \tag{25}$$

Here, MSE and Y are mean square error of system modeling and the original normal RAW signal, respectively. Figure 3 shows the error of bearing modeling based on the autoregressive learning technique and combination of mathematical system modeling and autoregressive learning technique. It is clear that the error rate of bearing modeling in the combination of MAT and autoregressive learning approach is lower than pure autoregressive learning approach. The mean square error of vibration normal signal modeling using the proposed modeling technique for training, validation, and testing is presented in Figure 4. Figure 4 illustrates that from the beginning of the training process, the training, validation, and test MSE curves sharply decreases within the first 12 epochs until they reach a MSE level near 3×10^{-4}. Then, for the next 40 epochs, some oscillations can be approximate and these curves converge to an Mean Square Error (MSE) level of around 1.2×10^{-4}. In the next section, the artificial intelligence-based observer is used to estimate the vibration signals for fault detection and identification in the bearing.

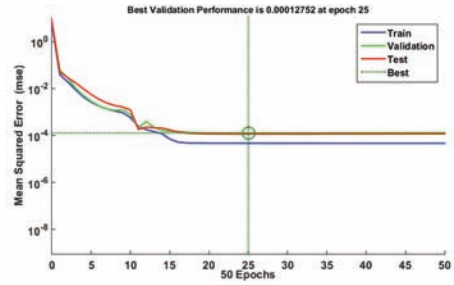

Figure 4 | Training, validation, and testing MSE curves during the training of the combination of mathematical system modeling and autoregressive learning approach.

4. ADAPTIVE FUZZY AUTOREGRESSIVE LEARNING LYAPUNOV OBSERVER FOR VIBRATION BEARING SIGNAL ESTIMATION

Based on Figure 1, the vibration signal of the bearing in the NRM was modeled by the combination of 5-DOF mathematical-based vibration signal modeling and autoregressive learning algorithm. Next, the state-space equation of vibration signal in NMR was extracted using Eq. (25). In this section, an artificial intelligence-based observer using a combination of a robust Lyapunov observer, autoregressive learning approach, and adaptive fuzzy technique is designed to estimate the vibration bearing signal. The following steps are used to design the artificial intelligence-based observer: (a) design the robust Lyapunov observer to estimate the normal vibration signal of bearing, (b) solve the challenge of the nonlinear part of signal estimation using the combination of autoregressive learning approach and Lyapunov observer, (c) to improve the flexibility, the combination of fuzzy algorithm, autoregressive learning approach, and Lyapunov observer is recommended, and (d) to increase the stability and reliability the combination of adaptive fuzzy, autoregressive learning approach, and Lyapunov observer is used in this work. Therefore, this section has two main sub-sections: (a) artificial intelligence-based observer based on the combination of Lyapunov observer, autoregressive learning approach, and adaptive fuzzy and (b) fault decision using the combination of residual signal generation and SVM.

4.1. Intelligence-Based Observer

Designing a nonlinear observer, especially with high stability and robustness, is a complicated and difficult task. Various methods have been introduced as observers, but in this section, we will introduce Lyapunov's technique. The Lyapunov based observer is described by Eq. [34]:

$$\begin{cases} \hat{X}_L(k+1) = [\alpha_{L_1}\hat{X}_L(k) + \alpha_{L_2}(\hat{Y}_L(k) - Y_{M-al}(k)] \\ \qquad\qquad + V_\gamma\left(e, X_{M-al}(k), f(k)\right) + \hat{f}_L(k) \\ \hat{Y}_L(k) = \left(\alpha_{L_3}\right)^T \hat{X}_L(k) \end{cases} \tag{26}$$

Here, $\hat{X}_L(k)$, $\hat{Y}_L(k)$, $V_\gamma\left(e, X_{M-al}(k), f(k)\right)$, $\hat{f}(k)$, and $\left(\alpha_{L_1}, \alpha_{L_2}, \alpha_{L_3}\right)$ are the estimation state of the Lyapunov-based observer for the

vibration signal of the bearing in the NRM, the estimation of the original vibration signal using the Lyapunov-based observer, the Lyapunov function, the estimation uncertainty using the Lyapunov-based observer, and the coefficients for tuning the Lyapunov-based observer in the NRM, respectively. The Lyapunov function is represented by the following equation:

$$V_\gamma\left(e, X_{M-al}(k), f(k)\right) = H_\gamma\left(e, X_{M-al}(k)\right) + \lambda_\gamma(e) f(k) \tag{27}$$

Here, $H_\gamma\left(e, X_{M-al}(k)\right)$ and $\lambda_\gamma(e)f(k)$ are the Hamilton–Jacobi inequality and continuously differentiable function of uncertainty, respectively. To modify the performance of the Lyapunov-based observer due to uncertain conditions, the following function is used:

$$\hat{f}_L(k+1) = \alpha_{L_2}(\hat{Y}_L(k) - Y_{M-al}(k)] + V_\gamma\left(e, X_{M-al}(k), f(k)\right) + \hat{f}_L(k) \tag{28}$$

The error of the original vibration estimation signal using the Lyapunov-based observer and the error of the uncertainty estimation using the Lyapunov-based observer are represented by the following mathematical definitions:

$$\begin{cases} \tilde{Y}_L(k) = Y_{M-al}(k) - \hat{Y}_L(k) \\ \tilde{f}_L(k) = f(k) - \hat{f}_L(k) \end{cases} \tag{29}$$

Here, $\tilde{Y}_L(k)$ and $\tilde{f}_L(k)$ are the error of the original vibration estimation signal using the Lyapunov-based observer and the error of the uncertainty estimation using the Lyapunov-based observer, respectively. This technique is robust and stable. Thus, the dynamics and gradient of estimation error for the Lyapunov-based observer are represented as follows:

$$\begin{aligned} \nabla e = {} & \alpha_{L_1}\hat{X}_L(k) + \alpha_{L_2}\left(\hat{Y}_L(k) - Y_{M-al}(k)\right) \\ & -\alpha_{\nabla e}\left(\hat{X}_L(k) - e(k), \left(\alpha_{L_3}\right)^T \hat{X}_L(k)\right) \end{aligned} \tag{30}$$

Here, ∇e and $\alpha_{\nabla e}$ are the dynamics of the estimation gradient error and the coefficient of gradient tuning, respectively. Therefore, the Lyapunov observer is input-to-state stable (ISS) if

$$\alpha_{L_2}\left(|e(k)|\right) \le V_\gamma\left(e, X_{M-al}(k), f(k)\right) \le \left(\alpha_{L_2} + \beta\right)\left(|e(k)|\right) \tag{31}$$

where $\left(\alpha_{L_2} + \beta\right)$ is a positive or negative value of the error coefficient representing the limitation of dynamics error. So, the stability of the Lyapunov-based observer is represented by the following definition:

$$\begin{aligned} & \alpha_{L_2}\left(|e(k)|\right) \le \nabla e . V_\gamma\left(e, X_{M-al}(k), f(k)\right) \\ & +\nabla_{\hat{X}_L(k)} . V_\gamma\left(e, X_{M-al}(k), f(k)\right) \le \left(\alpha_{L_2} + \beta\right)\left(|e(k)|\right) \end{aligned} \tag{32}$$

Here, $\nabla_{\hat{X}_L(k)}$ is a next state from the Lyapunov function point of view. The Lyapunov-based observer has the following challenges when estimating the bearing vibration signal and minimizing the error of estimation: (a) nonlinear behavior estimation of bearings extracted from vibration signal, (b) flexibility of Lyapunov-based approach, and (c) improvement of the accuracy and reliability of observer.

The nonlinear term of the Lyapunov-based observer is estimated by the autoregressive learning approach using the following mathematical definition:

$$\hat{Y}_{SVR}(k) = \sum_i \left(\alpha_i^+ - \alpha_i^-\right) K(x_i, x) + b \tag{33}$$

Here, $\hat{Y}_{SVR}(k)$ is the estimation of the nonlinear behavior of bearing vibration signal in NRMs using SVR. Therefore, the autoregressive learning Lyapunov scheme is defined by the following equations:

$$\begin{cases} \hat{X}_{LL}(k+1) = [\alpha_{L_1}\hat{X}_{LL}(k) + \alpha_{L_2}([\hat{Y}_{LL}(k) + \hat{Y}_{SVR}(k)] \\ \qquad -Y_{M-al}(k)] + V_\gamma\left(e, X_{M-al}(k), f(k)\right) + \hat{f}_{LL}(k) \\ \hat{Y}_{LL}(k) = \left(\alpha_{L_3}\right)^T \hat{X}_{LL}(k) \end{cases} \tag{34}$$

$$\begin{aligned} \hat{f}_{LL}(k+1) = {} & \alpha_{L_2}\left(\left[\hat{Y}_{LL}(k) + \hat{Y}_{SVR}(k)\right] - Y_{M-al}(k)\right) \\ & +V_\gamma\left(e, X_{M-al}(k), f(k)\right) + \hat{f}_{LL}(k) \end{aligned} \tag{35}$$

Here, $\hat{X}_{LL}(k)$, $\hat{Y}_{LL}(k)$, and $\hat{f}_{LL}(k)$ are the estimation state of autoregressive learning Lyapunov-based observer for bearing vibration signal in the NRM, the estimation of the original vibration signal using autoregressive learning Lyapunov-based observer, and the estimation uncertainty using autoregressive learning Lyapunov-based observer, respectively. The error of the original vibration estimation signal using autoregressive learning Lyapunov-based observer and the error of uncertainties estimation using autoregressive learning Lyapunov-based observer are represented by the following mathematical definitions:

$$\begin{cases} \tilde{Y}_{LL}(k) = Y_{M-al}(k) - \hat{Y}_{LL}(k) \\ \tilde{f}_{LL}(k) = f(k) - \hat{f}_{LL}(k) \end{cases} \tag{36}$$

where $\tilde{Y}_{LL}(k)$ and $\tilde{f}_{LL}(k)$ are the error of the original vibration estimation signal using autoregressive learning Lyapunov-based observer and the error of uncertainties estimation using autoregressive learning Lyapunov-based observer, respectively.

To address the next issue- improve the flexibility of the autoregressive learning Lyapunov-based observer, the fuzzy technique is recommended. The T-S fuzzy observer is used based on the following definition [35]:

$$\text{IF } \tilde{Y}(k) \text{ is } \Gamma_a \text{ THEN } \hat{f}_f(k+1) = \hat{f}_f(k) + L_f\left(f(k) - \hat{f}(k)\right) \tag{37}$$

Here, $\tilde{Y}(k)$, Γ_a, $\hat{f}_f$, and L_f are the error of output estimation, threshold values to detect the conditions, the estimation of uncertainty using the T-S fuzzy technique, and the coefficient for tuning the fuzzy technique, respectively. So, the mathematical function between the input and output based on the fuzzy technique is defined as follows:

$$\hat{f}_f(k+1) = \frac{\sum_k \hat{f}_f(k) \prod_{i=1}^{n} \mu\left(\tilde{Y}(k)\right)}{\sum_k \prod_{i=1}^{n} \mu\left(\tilde{Y}(k)\right)} \tag{38}$$

Here, $\mu\left(\tilde{Y}(k)\right)$ is the membership of the estimation error output (rules). Concerning Eq. (38), the fuzzy autoregressive learning Lyapunov-based observer is represented by the following techniques:

$$\begin{cases} \hat{X}_{fLL}(k+1) = [\alpha_{L_1}\hat{X}_{fLL}(k) + \alpha_{L_2}([\hat{Y}_{fLL}(k) + \hat{Y}_{SVR}(k)] \\ \qquad -Y_{M-al}(k)] + V_{\gamma}(e, X_{M-al}(k), f(k)) + \hat{f}_{fLL}(k) \\ \hat{Y}_{fLL}(k) = \left(\alpha_{L_3}\right)^T \hat{X}_{fLL}(k) \end{cases} \tag{39}$$

$$\begin{aligned} \hat{f}_{fLL}(k+1) = \alpha_{L_2}([\hat{Y}_{fLL}(k) + \hat{Y}_{SVR}(k)] - Y_{M-al}(k)) \\ +V_{\gamma}(e, X_{M-al}(k), f(k)) + \hat{f}_{fLL}(k) + \hat{f}_f(k) \end{aligned} \tag{40}$$

Here, $\hat{X}_{fLL}(k)$, $\hat{Y}_{fLL}(k)$, and $\hat{f}_{fLL}$ are the estimation state of the fuzzy autoregressive learning Lyapunov-based observer for bearing vibration signal in the NRM, the estimation of the original vibration signal using fuzzy autoregressive learning Lyapunov-based observer, and the estimation uncertainty using the fuzzy autoregressive learning Lyapunov-based observer, respectively. The error of the original vibration estimation signal using the fuzzy autoregressive learning Lyapunov-based observer and the error of the uncertainty estimation using the fuzzy autoregressive learning Lyapunov-based observer for the bearing are represented by the following mathematical definitions:

$$\begin{cases} \tilde{Y}_{fLL}(k) = Y_{M-al}(k) - \hat{Y}_{fLL}(k) \\ \tilde{f}_{fLL}(k) = f(k) - \hat{f}_{fLL}(k) \end{cases} \tag{41}$$

where $\tilde{Y}_{fLL}(k)$ and $\tilde{f}_{fLL}(k)$ are the error of the original vibration estimation signal using the fuzzy autoregressive learning Lyapunov-based observer and the error of the uncertainty estimation using the fuzzy autoregressive learning Lyapunov-based observer, respectively.

To address the final issue, improving the robustness and reliability of the fuzzy autoregressive learning Lyapunov-based observer, the adaptive procedure is recommended. Based on Eqs. (39) and (40), various coefficients for tuning the observer are defined in this algorithm such as $\alpha_{L_1}, \alpha_{L_2}, \alpha_{L_3}$, which are used to tune the estimation signal. To increase the reliability and robustness the adaptive fuzzy algorithm is recommended to online tuning the α_{L_3}. The updated coefficient is determined using the following definition:

$$\alpha_{L_{3-Update}} = \hat{f}_f(k) \times \alpha_{L_3} \tag{42}$$

Here, $\alpha_{L_{3-Update}}$ is the updated estimated signal coefficient using fuzzy adaptive algorithm. Based on Eq. (42), the adaptive fuzzy autoregressive learning Lyapunov-based observer is represented by the following functions:

$$\begin{cases} \hat{X}_{AfLL}(k+1) = [\alpha_{L_1}\hat{X}_{AfLL}(k) + \alpha_{L_2}([\hat{Y}_{AfLL}(k) + \hat{Y}_{SVR}(k)] \\ \qquad -Y_{M-al}(k)] + V_{\gamma}(e, X_{M-al}(k), f(k)) + \hat{f}_{AfLL}(k) \\ \hat{Y}_{AfLL}(k) = \left(\alpha_{L_{3-Update}}\right)^T \hat{X}_{AfLL}(k) \end{cases} \tag{43}$$

$$\begin{aligned} \hat{f}_{AfLL}(k+1) = \alpha_{L_2}([\hat{Y}_{AfLL}(k) + \hat{Y}_{SVR}(k)] - Y_{M-al}(k)) \\ +\hat{f}_f(k) + V_{\gamma}(e, X_{M-al}(k), f(k)) + \hat{f}_{AfLL}(k) \end{aligned} \tag{44}$$

Here, $\hat{X}_{AfLL}(k)$, $\hat{Y}_{AfLL}(k)$, and $\hat{f}_{AfLL}$ are the estimation state of the adaptive fuzzy autoregressive learning Lyapunov-based observer for the bearing vibration signal in the NRM the estimation of the original vibration signal using the adaptive fuzzy autoregressive learning Lyapunov-based observer, and the estimation uncertainty using the adaptive fuzzy autoregressive learning Lyapunov-based observer, respectively. The error of uncertainty estimation using the adaptive fuzzy autoregressive learning Lyapunov-based observer for the bearing is represented by the following mathematical definition:

$$\tilde{f}_{AfLL}(k) = f(k) - \hat{f}_{AfLL}(k) \tag{45}$$

where $\tilde{f}_{AfLL}(k)$ is the error of uncertainty estimation using the adaptive fuzzy autoregressive learning Lyapunov-based observer. In summary, this section consisted of three main parts. First, the robust Lyapunov-based observer is designed. To improve the uncertainty estimation accuracy, the autoregressive learning Lyapunov-based observer was designed in the second stage. Next, the fuzzy autoregressive learning Lyapunov-based observer was introduced to improve the flexibility and accuracy of the previous approach. Finally, the adaptive fuzzy autoregressive learning Lyapunov-based observer (intelligence-based observer) was introduced to improve the power of reliability and stability of the fault identification technique. For fault detection and identification, the next section focuses on generating the residual signal and implementing the SVM.

4.2. Fault Detection and Identification

As shown in Figure 1, the normal signal was approximated using a combination of MATs and the autoregressive learning approach. After that, the adaptive fuzzy autoregressive learning Lyapunov-based observer (intelligence-based observer) was designed to improve the power of the estimation technique. In this section, the residual signal is determined, which is the difference between the original and estimated signals. Based on this definition, the residual signal is represented by the following technique:

$$R_{AfLL} = Y_{M-al}(k) - \hat{Y}_{AfLL}(k) \tag{46}$$

Here, R_{AfLL} is the residual signal based on the adaptive fuzzy autoregressive learning Lyapunov-based observer. Moreover, the SVM is used to detect and identify the types of faults in the bearing. To characterize the bearing residual signals by statistical features, first, we divide the bearing residual signals into equally sized windows. In Tables 1 and 2, the rotational speed varies between 1730–1797 RPM or 28–30 rotations per second [31]. Moreover, the frequency of the sampling rate is adjusted to 48 kHz. To cover all information in every rotation, 1600 samples are required. On the other hand, the vibration CWRU bearing signal length is 150000 samples. Thus, 100 windows are selected for CWRU bearing dataset.

After resampling the residual signals of the bearing, statistical features such as the RMS are extracted from the resampled residual signals. The following equation represents the RMS of the residual signals:

$$R_{AfLL_{RMS}} = \sqrt{\left(\frac{1}{N}\sum_{i=1}^{N}\left(R_{AfLL}(i)\right)^2\right)} \tag{47}$$

Here, $R_{AfLL_{RMS}}$, N, and $R_{AfLL}(i)$ are the RMS value of the $(i)^{th}$ window, the number of windows, and the $(i)^{th}$ window of the original bearing signal, respectively. The nonlinear SVM using the kernel trick is defined by Eqs. [32,33]:

$$\theta_a = \sum_a \left(\alpha_a^+ - \alpha_a^-\right) K\left(\tilde{f}_{AfLL}(k), \hat{f}_{AfLL}(k)\right) + b_\theta \tag{48}$$

Here, θ_a, $\left(\alpha_a^+, \alpha_a^-\right)$, $K\left(\tilde{f}_{AfLL}(k), \hat{f}_{AfLL}(k)\right)$, and b_θ are the threshold nonlinear area using the SVM technique, the Lagrange coefficients, the kernel, and the bias, respectively. The Gaussian function to design the nonlinear SVM is defined by the following function:

$$K\left(\tilde{f}_{AfLL}(k), \hat{f}_{AfLL}(k)\right) = e^{\left(-\frac{1}{2\sigma^2}\|\tilde{f}_{AfLL}(k), \hat{f}_{AfLL}(k)\|^2\right)} \tag{49}$$

Here, σ is the variance. Furthermore, the bias is represented by the following equation:

$$b_\theta = \frac{1}{|S_\theta|} \times \sum_{s \in S_\theta} \begin{bmatrix} \hat{Y}_{S_\theta} - \sum_{a \in S} \left(\alpha_a^+ - \alpha_a^-\right) \\ \times K\left(\tilde{f}_{AfLL}(k), \hat{f}_{AfLL}(k)\right) - \varepsilon_\theta \\ \times sign\left(\theta_a^+ - \theta_a^-\right) \end{bmatrix} \tag{50}$$

where $\hat{Y}_{S_\theta}$ and S_θ are the bearing vibration signal of the support vector and the support vector, respectively. The support vector is defined by the following equation:

$$S_\theta = \{a | 0 < \alpha_a^+ + \alpha_a^- < \delta_\theta\} \tag{51}$$

Here, δ_θ is a constant. To solve Eq. (48), $\left(\alpha_a^+ + \alpha_a^-\right)$ needs to determined. To determine $\left(\alpha_a^+ + \alpha_a^-\right)$, the following technique is recommended:

$$\min \sum_a \sum_b \left(\alpha_a^+ - \alpha_a^-\right)\left(\alpha_a^+ - \alpha_a^-\right) K\left(\tilde{f}_{AfLL}(k), \hat{f}_{AfLL}(k)\right) \tag{52}$$

If $K\left(\tilde{f}_{AfLL}(k), \hat{f}_{AfLL}(k)\right)$ is defined as γ_{ab},

$$\min \sum_a \sum_a \alpha_a^+ \alpha_a^+ \gamma_{ab} - \alpha_a^- \alpha_a^+ \gamma_{ab} - \alpha_a^+ \alpha_a^- \gamma_{ab} + \alpha_a^- \alpha_a^- \gamma_{ab} \tag{53}$$

After specifying the threshold expanse using the SVM, the fault can be detected and its type can be specified. Algorithm Algorithm 1 represents the proposed technique, which is a combination of intelligence-based observer and SVM for fault detection and identification of bearing systems.

Algorithm 1: Intelligence-based observer and SVM for fault detection and identification in the bearing.

Step 1: Signal Modeling

1: Approximate the bearing function from the vibration signals using MATs. (10)

Detail

1.1 Solve Θ_b. (4)

1.2 Solve Θ_i. (8)

1.3 Solve Θ_o. (9)

1.4 $\Delta \leftarrow \Theta_b + \Theta_i + \Theta_o$. (3)

1.5 Compute $X_M(k+1) \leftarrow \alpha_M \times X_M(k) + \Delta$. (10)

1.6 Compute $Y_M(k) \leftarrow (\alpha_G)^T \times X_M(k)$. (10)

2: Approximate the bearing function from normal vibration signal using autoregressive technique. (11)

Detail

2.1 Calculate $e_a(k) \leftarrow Y_a(k+1) - Y_a(k)$. (12)

2.2 Compute $X_a(k+1) \leftarrow [\alpha_a X_a(k) + \alpha_{ai} U_{ai}(k)] + e_a(k) + f(k)$ (11)

2.3 Compute $Y_a(k) \leftarrow (\alpha_o)^T X_a(k)$. (11)

3: Improve the robustness of Eq. (11) using autoregressive algorithm with the Laguerre filter. (13)

Detail

3.1 Calculate $e_{la}(k) \leftarrow Y_{la}(k+1) - Y_{la}(k)$. (14)

3.2 Calculate $Y_{la}(k) \leftarrow (\alpha_o)^T X_{la}(k)$ (13)

3.3 Calculate $X_{la}(k+1) \leftarrow [\alpha_a X_{la}(k) + \alpha_{ai} U_{ai}(k) + \alpha_{lao} Y_{la}(k)] + e_{la}(k) + f(k)$ (13)

4: Increase the accuracy and nonlinearity of Eq. (13) using the autoregressive learning approach. (23)

Detail

4.1 Compute $K(x_i, x) \leftarrow e^{\left(-\frac{1}{2\sigma^2}\|x_i - x\|^2\right)}$ (16)

4.2 Calculate $S = \left\{i | 0 < \alpha_i^+ + \alpha_i^- < \delta\right\}$ (22)

4.3 Compute $b \leftarrow \frac{1}{|S|} \sum_{s \in S} \left[Y_s - \sum_{i \in S} \left(\alpha_i^+ - \alpha_i^-\right) \times K\left(x_i, x_S\right) - \varepsilon \times sign \alpha_i^+ - \alpha_i^- \right]$ (21)

4.4 Calculate $Y_{SVR} \leftarrow \sum_i \left(\alpha_i^+ - \alpha_i^-\right) K\left(x_i, x\right) + b$ (15)

4.5 Compute $e_{al}(k) \leftarrow Y_{al}(k+1) - Y_{al}(k)$ (24)

4.6 Calculate $X_{al}(k+1) = [\alpha_a X_{al}(k) + \alpha_{ai} U_{ai}(k) + \alpha_{lao}(Y_{la}(k) + Y_{SVR}(k))] + e_{al}(k) + f(k)]$ (23)

4.7 Compute $Y_{al}(k) = (\alpha_o)^T X_{al}(k)$ (23)

Step 2: Signal Estimation

5: Signal estimation using robust Lyapunov-based observer. (26–28)

Detail

5.1 Compute $V_\gamma(e, X_{M-al}(k), f(k)) \leftarrow H_\gamma(e, X_{M-al}(k)) + \lambda_\gamma(e) f(k)$ (27)

5.2 Calculate $\hat{f}_L(k+1) \leftarrow \alpha_{L_2}(\hat{Y}_L(k) - Y_{M-al}(k)] + V_\gamma(e, X_{M-al}(k), f(k)) + \hat{f}_L(k)$ (28)

5.3 Compute $\hat{X}_L(k+1) \leftarrow [\alpha_{L_1} \hat{X}_L(k) + \alpha_{L_2}(\hat{Y}_L(k) - Y_{M-al}(k)] + V_\gamma(e, X_{M-al}(k), f(k)) + \hat{f}_L(k)$ (26)

5.4 Calculate $\hat{Y}_L(k) \leftarrow (\alpha_{L_3})^T \hat{X}_L(k)$ (26)

6: Estimate the nonlinearity of robust Lyapunov-based observer using autoregressive learning Lyapunov-based observer. (34,35)

Detail

6.1 Compute $\hat{Y}_{SVR}(k) \leftarrow \sum_i \left(\alpha_i^+ - \alpha_i^-\right) K(x_i, x) + b$ (33)

6.2 Calculate $\hat{f}_{LL}(k+1) \leftarrow \alpha_{L_2}([\hat{Y}_{LL}(k) + \hat{Y}_{SVR}(k)] - Y_{M-al}(k)) + V_\gamma(e, X_{M-al}(k), f(k)) + \hat{f}_{LL}(k)$ (35)

6.3 Solve $\hat{X}_{LL}(k+1) \leftarrow [\alpha_{L_1} \hat{X}_{LL}(k) + \alpha_{L_2}([\hat{Y}_{LL}(k) + \hat{Y}_{SVR}(k)] - Y_{M-al}(k)] + V_\gamma(e, X_{M-al}(k), f(k)) + \hat{f}_{LL}(k)$ (34)

6.4 Compute $\hat{Y}_{LL}(k) \leftarrow (\alpha_{L_3})^T \hat{X}_{LL}(k)$ (34)

7: Increase the accuracy and flexibility using the fuzzy autoregressive learning Lyapunov-based observer. (39,40)

Detail

7.1 Calculate $\hat{f}_f(k+1) \leftarrow \dfrac{\sum_k \hat{f}_f(k) \prod_{i=1}^{n} \mu\left(\tilde{Y}(k)\right)}{\sum_k \prod_{i=1}^{n} \mu\left(\tilde{Y}(k)\right)}$ (38)

7.2 Solve $\hat{f}_{fLL}(k+1) \leftarrow \alpha_{L_2}([\hat{Y}_{fLL}(k) + \hat{Y}_{SVR}(k)] - Y_{M-al}(k)) + V_\gamma(e, X_{M-al}(k), f(k)) + \hat{f}_{fLL}(k) + \hat{f}_f(k)$ (40)

7.3 Compute $\hat{X}_{fLL}(k+1) \leftarrow [\alpha_{L_1} \hat{X}_{fLL}(k) + \alpha_{L_2}([\hat{Y}_{fLL}(k) + \hat{Y}_{SVR}(k)] - Y_{M-al}(k)] + V_\gamma(e, X_{M-al}(k), f(k)) + \hat{f}_{fLL}(k)$ (39)

7.4 Calculate $\hat{Y}_{fLL}(k) \leftarrow (\alpha_{L_3})^T \hat{X}_{fLL}(k)$ (39)

8: Increase the stability, accuracy, and robustness using an adaptive fuzzy autoregressive learning Lyapunov-based observer. (43,44)

Detail

8.1 Solve $\alpha_{L_{3-Update}} \leftarrow \hat{f}_f(k) \times \alpha_{L_3}$ (42)

8.2 Compute $\hat{f}_{AfLL}(k+1) \leftarrow \alpha_{L_2}([\hat{Y}_{AfLL}(k) + \hat{Y}_{SVR}(k)] - Y_{M-al}(k)) + \hat{f}_f(k) + V_\gamma(e, X_{M-al}(k), f(k)) + \hat{f}_{AfLL}(k)$ (44)

8.3 Calculate $\hat{X}_{AfLL}(k+1) \leftarrow [\alpha_{L_1}\hat{X}_{AfLL}(k) + \alpha_{L_2}([\hat{Y}_{AfLL}(k) + \hat{Y}_{SVR}(k)] - Y_{M-al}(k)] + V_\gamma(e, X_{M-al}(k), f(k)) + \hat{f}_{AfLL}(k)$ (43)

8.4 Solve $\hat{Y}_{AfLL}(k) \leftarrow \left(\alpha_{L_{3-Update}}\right)^T \hat{X}_{AfLL}(k)$ (43)

Step 3: Decision Making

9: Generate the residual signal. (46)

10: Resample and extract the RMS feature from residual signal. (47)

11: Fault detection and classification using SVM. (48)

Detail

11.1 Compute $K\left(\tilde{f}_{AfLL}(k), \hat{f}_{AfLL}(k)\right) \leftarrow e^{\left(-\frac{1}{2\sigma^2}\|\tilde{f}_{AfLL}(k), \hat{f}_{AfLL}(k)\|^2\right)}$ (49)

11.2 Calculate $b_\theta = \frac{1}{|S_\theta|} \times \sum_{s \in S_\theta} \left[\begin{array}{l} \hat{Y}_{S_\theta} - \sum_{a \in S} (\alpha_a^+ - \alpha_a^-) \times \\ K\left(\tilde{f}_{AfLL}(k), \hat{f}_{AfLL}(k)\right) - \varepsilon_\theta \\ \times sign\left(\theta_a^+ - \theta_a^-\right) \end{array} \right]$ (50)

11.3 Find $S_\theta = \{a | 0 < \alpha_a^+ + \alpha_a^- < \delta_\theta\}$ (51)

11.4 Compute $\min \sum_a \sum_b (\alpha_a^+ - \alpha_a^-)(\alpha_a^+ - \alpha_a^-) K\left(\tilde{f}_{AfLL}(k), \hat{f}_{AfLL}(k)\right)$ (52)

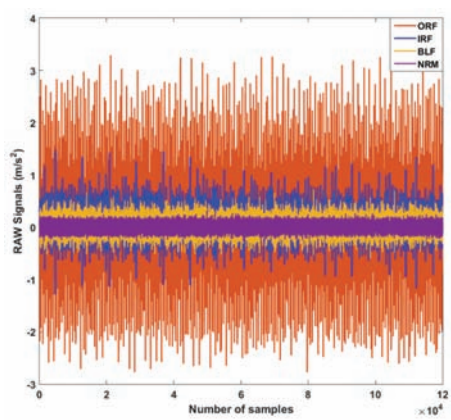

Figure 5 Different classes from Case Western Reverse University (CWRU) dataset for 0-hp and 0.007-inch crack.

5. RESULTS

To test the power of fault detection and identification, the CWRU dataset is used in this work. This vibration dataset has four classes: NRM, BLF, IRF, and ORF. Table 3 shows the window characterizations for estimated and verification signals from the CWRU bearing vibration dataset. Figure 5 illustrates these classes when the torque load and crack size are 0-hp and 0.007-inch, respectively.

To test the effectiveness of the bearing fault classification using the intelligence-based observer + SVM, this method is validated and compared with two state-of-the-art techniques: the autoregressive learning Lyapunov-based approach + SVM and the Lyapunov-based technique + SVM. Figures 6–8 illustrate the residual signals

Table 3 Case Western Reverse University (CWRU) window characterization for training and testing: CWRU data.

Classes	Number of Samples
Samples per state	100
Samples per classes	4*100 = 400
Training samples per state	60
Training samples per classes	240
Validating samples per state	15
Validating samples per classes	60
Testing samples per state	25
Testing samples per state	100

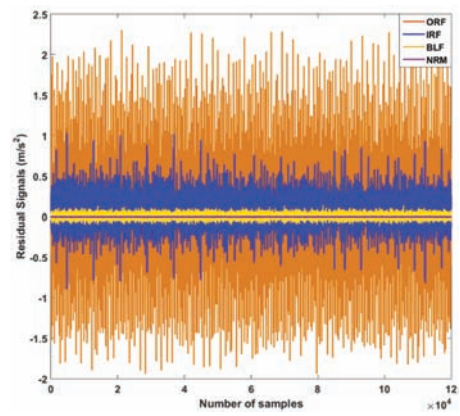

Figure 6 Residual signals using proposed intelligence-based observer.

for the four classes using the intelligence-based observer, autoregressive learning Lyapunov-based approach, and Lyapunov-based technique, respectively.

Based on these figures, it can be seen that the intelligence-based observer has better separability than the autoregressive learning Lyapunov-based approach and Lyapunov-based technique. Based on Figures 6 and 7, the detectability in the autoregressive learning Lyapunov-based approach is better than that of the Lyapunov-based technique. Figure 9 compares the RMS values of the residual signals calculated by the intelligence-based observer, autoregressive learning Lyapunov-based approach, and Lyapunov-based technique. According to this figure, fault detection accuracy, which is the discrimination of normal from abnormal signals, is exceptional in all three algorithms.

As shown in these figures, the classification accuracy for the proposed algorithm (intelligence-based observer) is better than those of the other two methods. The main problem of fault identification in the autoregressive learning Lyapunov-based approach and Lyapunov-based technique is related to anomaly identification for inner and outer defects.

The K-fold cross-validation is used to validate the accuracy and precision of the intelligent-based observer + SVM (proposed scheme), autoregressive learning Lyapunov-based observer + SVM, and Lyapunov-based observer + SVM, respectively. To produce the stable results, the K in the experiment is 5 and the average of accuracy shows in Tables 4–6 and Figures 10–12.

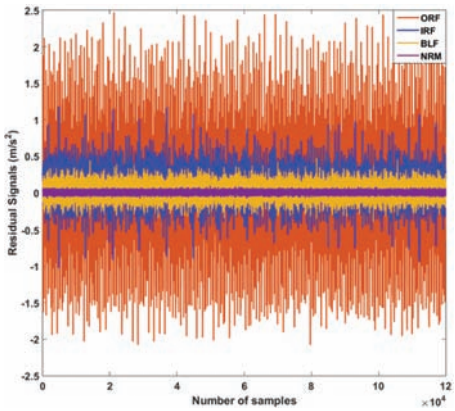

Figure 7 | Residual signals using autoregressive learning Lyapunov-based approach.

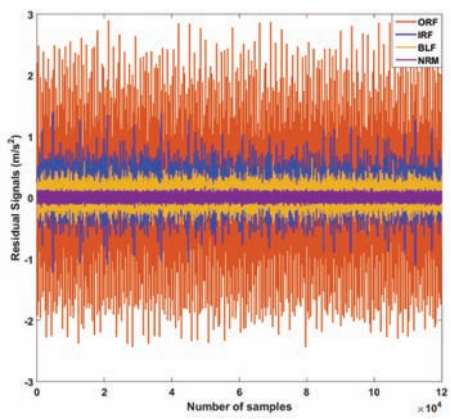

Figure 8 | Residual signals using Lyapunov-based technique.

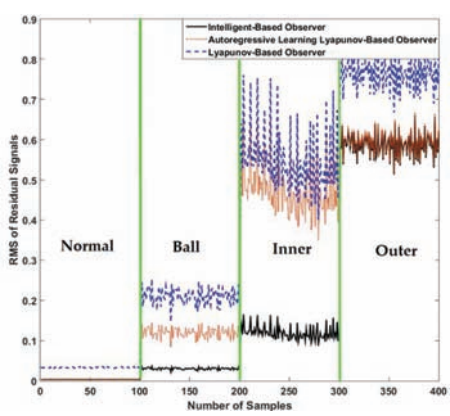

Figure 9 | Root mean square (RMS) of residual signals using proposed intelligence-based observer, autoregressive learning Lyapunov-based approach, and Lyapunov-based technique.

Tables 4–6 illustrate the power of fault identification using the intelligence-based observer, autoregressive learning Lyapunov-based approach, and Lyapunov-based technique when the torque load varies between 0-hp and 3-hp.

Based on the above tables, the fault identification accuracy of the proposed scheme is much better than those of the other two methods. In addition, the average accuracy of the intelligence-based observer + SVM is about 97.1%, whereas in the autoregressive learning Lyapunov-based approach + SVM and Lyapunov-based technique + SVM it is 92.8% and 91%, respectively. Thus, the proposed algorithm improved the average fault identification accuracy by 4.3% and 6.1% compared to the autoregressive learning Lyapunov-based approach + SVM and Lyapunov-based technique + SVM, respectively. Figures 10–12 show the confusion matrices of these algorithms. Based on these

Intelligent Based Observer

True Class \ Predicted Class	NRM%	BLF%	IRF%	ORF%
NRM%	100	0	0	0
BLF%	1%	94.8	4.2	0
IRF%	0	2	95.4	2.6
ORF%	0	0	2	98
Average of Precision	99%	98%	94%	97.4%

Figure 10 | Confusion matrix to calculate the average fault diagnosis accuracy and precision using intelligent-based observer + support vector machine (SVM) for various crack sizes (0.007-inch, 0.014-inch, and 0.021-inch) and different torque loads (0-hp, 1-hp, 2-hp, and 3-hp).

Autoregressive Learning Lyapunov-based Observer

True Class \ Predicted Class	NRM%	BLF%	IRF%	ORF%
NRM%	100	0	0	0
BLF%	2%	93	4	1
IRF%	0	3	90	7
ORF%	1	3	8	88
Average of Precision	97%	94%	88.2%	91.6%

Figure 11 | Confusion matrix to calculate the average fault diagnosis accuracy and precision using autoregressive learning Lyapunov-based observer + support vector machine (SVM) for various crack sizes (0.007-inch, 0.014-inch, and 0.021-inch) and different torque loads (0-hp, 1-hp, 2-hp, and 3-hp).

Lyapunov-based Observer

True Class \ Predicted Class	NRM%	BLF%	IRF%	ORF%
NRM%	100	0	0	0
BLF%	4	91	5	0
IRF%	1	5	87	7
ORF%	2	3	9	86
Average of Precision	92.5%	92%	86.1%	92.4%

Figure 12 | Confusion matrix to calculate the average fault diagnosis accuracy and precision using Lyapunov-based observer + support vector machine (SVM) for various crack sizes (0.007-inch, 0.014-inch, and 0.021-inch) and different torque loads (0-hp, 1-hp, 2-hp, and 3-hp).

Table 4 The average fault diagnosis accuracy using intelligence-based observer + SVM for crack sizes of 0.007-inch, 0.014-inch, and 0.021-inch.

Algorithm	Intelligence-Based Observer + SVM			
Torque Load	**0-hp (%)**	**1-hp (%)**	**2-hp (%)**	**3-hp (%)**
NRM	100	100	100	100
BLF	97.3	97.3	91.3	93.3
IRF	94.7	93.3	98.7	94.7
ORF	98.3	96	100	98.3
Average	97.6	96.7	97.5	96.6

SVM, support vector machine; NRM, normal condition; BLF, ball fault; IRF, inner race fault; ORF, outer race fault.

Table 5 The average fault diagnosis accuracy using autoregressive learning Lyapunov-based approach + SVM for crack sizes of 0.007-inch, 0.014-inch, and 0.021-inch.

Algorithm	Autoregressive learning Lyapunovbased observer + SVM			
Torque Load	**0-hp (%)**	**1-hp (%)**	**2-hp (%)**	**3-hp (%)**
NRM	100	100	100	100
BLF	93	91	97.3	90.7
IRF	88	92	92	88
ORF	90.3	84.3	89.7	88
Average	92.8	91.8	94.8	91.7

SVM, support vector machine; NRM, normal condition; BLF, ball fault; IRF, inner race fault; ORF, outer race fault.

Table 6 The average fault diagnosis accuracy using Lyapunov-based observer + SVM for crack sizes of 0.007-inch, 0.014-inch, and 0.021-inch.

Algorithm	Lyapunov-Based Observer + SVM			
Torque Load	**0-hp (%)**	**1-hp (%)**	**2-hp (%)**	**3-hp (%)**
NRM	100	100	100	100
BLF	89.7	93.3	92.7	88.3
IRF	82	88	88	90
ORF	87	83	86	88
Average	89.7	91	91.7	91.6

SVM, support vector machine; NRM, normal condition; BLF, ball fault; IRF, inner race fault; ORF, outer race fault.

figures, these confusion matrices are the average accuracy and precision for various crack sizes and different torque loads. Regarding these figures, it is clear that the average accuracy and precision for the proposed scheme is better than the other methods. The range of misclassification in the proposed method is less than the others.

6. CONCLUSION

The principal purpose of this work was to solve the challenge of identification and classification of faults in a bearing. The combination of mathematical and autoregressive learning approaches, an intelligence-based observer, and the SVM were considered to address this issue. This approach consists of four main steps. First, the signal was modeled in normal operation using a combination of mathematical vibration signal modeling and autoregressive learning vibration signal approximation techniques. After modeling the normal vibration signal, the signal was estimated using a combination of the modern control algorithm and machine learning techniques. To approximate the signal, first, the robust Lyapunov-based technique was selected, and in later stages, this procedure was modified. Next, the problem of nonlinear parameters was solved by combining the Lyapunov-based observer method with an autoregressive learning scheme. To increase the flexibility, the autoregressive learning Lyapunov-based observation technique was combined with a fuzzy logic approach. Finally, to improve the accuracy and increase the robustness, the fuzzy autoregressive learning Lyapunov-based observer was combined with the adaptive technique. In the final step, the fault was classified and identified by the SVM. The proposed algorithm improved the average fault identification accuracy by 3.9% and 5.2% compared to the autoregressive learning Lyapunov-based approach and Lyapunov-based observer, respectively.

CONFLICTS OF INTEREST

The authors declare no conflict of interest.

AUTHORS' CONTRIBUTIONS

All of the authors contributed equally to the conception of the idea, the design of experiments, the analysis and interpretation of results, and the writing of the manuscript. Writing—original draft preparation, F.P. and J.-M.K.; writing—review and editing, F.P. and J.-M.K. All authors have read and agreed to the published version of the manuscript.

FUNDING STATEMENT

This work was supported by the Korea Institute of Energy Technology Evaluation and Planning (KETEP) and the Ministry of Trade, Industry & Energy (MOTIE) of the Republic of Korea (No. 20192510102510).

ACKNOWLEDGMENTS

This work was supported by the Korea Institute of Energy Technology Evaluation and Planning (KETEP) and the Ministry of Trade, Industry & Energy (MOTIE) of the Republic of Korea (No. 20192510102510).

REFERENCES

[1] M.L. Adams, Analysis of Rolling Element Bearing Faults in Rotating Machinery: Experiments, Modeling, Fault Detection and Diagnosis, Case Western Reserve University, Cleveland, OH, USA, 2001.

[2] C. Cecati, A survey of fault diagnosis and fault-tolerant techniques—part II: fault diagnosis with knowledge-based and hybrid/active approaches, IEEE Trans. Ind. Electron. 62 (2015), 3768–3774.

[3] Z. Gao, C. Cecati, S.X. Ding, A survey of fault diagnosis and fault-tolerant techniques—part I: fault diagnosis with model-based and signal-based approaches, IEEE Trans. Ind. Electron. 62 (2015), 3757–3767.

[4] Z. Liu, T. Liu, J. Han, S. Bu, X. Tang, M. Pecht, Signal model-based fault coding for diagnostics and prognostics of analog electronic circuits, IEEE Trans. Ind. Electron. 64 (2016), 605–614.

[5] W. Ahmad, S.A. Khan, J.-M. Kim, A hybrid prognostics technique for rolling element bearings using adaptive predictive models, IEEE Trans. Ind. Electron. 65 (2017), 1577–1584.
[6] A. Glowacz, Acoustic-based fault diagnosis of commutator motor, Electronics. 7 (2018), 299.
[7] Z. Huo, Y. Zhang, L. Shu, M. Gallimore, A new bearing fault diagnosis method based on fine-to-coarse multiscale permutation entropy, laplacian score and SVM, IEEE Access. 7 (2019), 17050–17066.
[8] Z. Chu, F. Meng, D. Zhu, C. Luo, Fault reconstruction using a terminal sliding mode observer for a class of second-order MIMO uncertain nonlinear systems, ISA Trans. 97 (2020), 67–75.
[9] F. Chu, W. Lu, Experimental observation of nonlinear vibrations in a rub-impact rotor system, J. Sound Vib. 283 (2005), 621–643.
[10] X. Xue, J. Zhou, A hybrid fault diagnosis approach based on mixed-domain state features for rotating machinery, ISA Trans. 66 (2017), 284–295.
[11] H.O. Ahmed, A.K. Nandi, Three-stage hybrid fault diagnosis for rolling bearings with compressively sampled data and subspace learning techniques, IEEE Trans. Ind. Electron. 66 (2018), 5516–5524.
[12] S. Zhou, S. Qian, W. Chang, Y. Xiao, Y. Cheng, A novel bearing multi-fault diagnosis approach based on weighted permutation entropy and an improved SVM ensemble classifier, Sensors. 18 (2018), 1934.
[13] F. Piltan, A.E. Prosvirin, M. Sohaib, B. Saldivar, J.-M. Kim, An SVM-based neural adaptive variable structure observer for fault diagnosis and fault-tolerant control of a robot manipulator, Appl. Sci. 10 (2020), 1344.
[14] F. Piltan, A.E. Prosvirin, I. Jeong, K. Im, J.-M. Kim, Rolling-element bearing fault diagnosis using advanced machine learning-based observer, Appl. Sci. 9 (2019), 5404.
[15] K. Bouzrara, T. Garna, J. Ragot, H. Messaoud, Decomposition of an ARX model on Laguerre orthonormal bases, ISA Trans. 51 (2012), 848–860.
[16] A. Forrai, System identification and fault diagnosis of an electromagnetic actuator, IEEE Trans. Control Syst. Technol. 25 (2016), 1028–1035.
[17] C. Mishra, A. Samantaray, G. Chakraborty, Ball bearing defect models: a study of simulated and experimental fault signatures, J. Sound Vib. 400 (2017), 86–112.
[18] F. Piltan, J.-M. Kim, Nonlinear extended-state ARX-Laguerre PI observer fault diagnosis of bearings, Appl. Sci. 9 (2019), 888.
[19] F.K. Gündoğdu, C. Kahraman, A novel fuzzy TOPSIS method using emerging interval-valued spherical fuzzy sets, Eng. Appl. Artif. Intell. 85 (2019), 307–323.
[20] R.-E. Precup, T.-A. Teban, A. Albu, A.-B. Borlea, I.A. Zamfirache, E.M. Petriu, Evolving fuzzy models for prosthetic hand myoelectric-based control, IEEE Trans. Instrum. Meas. 69 (2020), 4625–4636.
[21] M.U. Ahmed, S. Brickman, A. Dengg, N. Fasth, M. Mihajlovic, J. Norman, A machine learning approach to classify pedestrians' events based on IMU and GPS, Int. J. Artif. Intell. 17 (2019), 154–167.
[22] R.-E. Precup, T.-A. Teban, A. Albu, A.-B. Borlea, I.A. Zamfirache, E.M. Petriu, Evolving fuzzy models for prosthetic hand myoelectricbased control using weighted recursive least squares algorithm for identification, in Proceeding of IEEE International Symposium on Robotic and Sensors Environments (ROSE), Ottawa, Canada, 2019, pp. 164–169.
[23] H. Cao, S. Sun, K. Zhang, Modified EMG-based handgrip force prediction using extreme learning machine, Soft Comput. 21 (2017), 491–500.
[24] R.-E. Precup, T.-A. Teban, A. Albu, Evolving fuzzy and neural network models of finger dynamics for prosthetic hand myoelectricbased control, in Proceeding of 11th 11th International Conference on Electronics, Computers and Artificial Intelligence (ECAI), Pitesti, Romania, 2019, pp. 1–8.
[25] V. Mien, H.-J. Kang, K.-S. Shin, Backstepping quasi-continuous high-order sliding mode control for a Takagi–Sugeno fuzzy system with an application for a two-link robot control, Proc. Inst. Mech. Eng. Part C J. Mech. Eng. Sci. 228 (2014), 1488–1500.
[26] V. Mien, P. Franciosa, D. Ceglarek, Fault diagnosis and fault-tolerant control of uncertain robot manipulators using high-order sliding mode, Math. Probl. Eng. 2016 (2016), 1–14.
[27] H. Yang, S. Yin, Reduced-order sliding-mode-observer-based fault estimation for Markov jump systems, IEEE Trans. Autom. Control. 64 (2019), 4733–4740.
[28] F. Piltan, J.-M. Kim, Bearing fault diagnosis by a robust higher-order super-twisting sliding mode observer, Sensors. 18 (2018), 1128.
[29] F. Piltan, J.-M. Kim, Bearing fault diagnosis using an extended variable structure feedback linearization observer, Sensors. 18 (2018), 4359.
[30] T. Najeh, C.B. Njima, T. Garna, J. Ragot, Input fault detection and estimation using PI observer based on the ARX-Laguerre model, Int. J. Adv. Manuf. Technol. 90 (2017), 1317–1336.
[31] Bearing Data Center, Case Western Reserve University seeded fault test data, 2020. https://csegroups.case.edu/bearingdatacenter/pages/welcome-case-western-reserve-university-bearing-data-center-website
[32] G.C. Wu, D. Baleanu, W.H. Luo, Lyapunov functions for Riemann–Liouville-like fractional difference equations, Appl. Math. Comput. 314 (2017), 228–236.
[33] C.-W. Hsu, C.-C. Chang, C.-J. Lin, A practical guide to support vector classification, 2010. https://www.researchgate.net/
[34] L.M. Manevitz, M. Yousef, One-class SVMs for document classification, J. Mach. Learn. Res. 2 (2001), 139–154.
[35] W.-B. Xie, C.H. Lim, J. Zhang, L. Huang, New approaches to observer design and stability analysis for T–S fuzzy system with multiplicative noise, J. Frankl. Inst. 354 (2017), 887–901.